Power System Inertia Estimation: Review of Methods and the Impacts of Converter-Interfaced Generations

Bendong Tan, Junbo Zhao, Marcos Netto, Venkat Krishnan, Vladimir Terzija, Yingchen Zhang

***Abstract*—Understanding and quantifying the inertia of power systems with the integration of converter-interfaced generation (CIG) plays an essential role in the safe transition to a future low-inertia scenario. This paper provides a comprehensive summary of inertia definitions for both synchronous generators and CIGs as well as their corresponding estimation methods. In particular, the estimation methods are categorized as model-based and measurement-based approaches considering both small and large disturbances. The advantages and disadvantages of different methods are carefully discussed. This paper also offers for the first time a framework to quantify the virtual inertia of CIGs at the component and aggregation levels, an open problem in the literature. Finally, future directions for inertia estimation are identified and discussed. This significantly benefits the design of appropriate control and protection schemes in achieving a more reliable, secure, and resilient power system.**

***Index Terms*— Converter interfaced generations, frequency stability, inertia estimation, low-inertia system, power system stability, synchronous generators, virtual inertia emulation.**

I. Introduction

In the past decades, increasing penetration of converter-interfaced generation (CIGs)—such as photovoltaics (PVs), and wind—have been integrated into power systems to replace traditional synchronous generators (SGs) [1]. In 2019, the total wind capacity was 650.8 GW globally [2] and that of PV was 580.1 GW [3]. However, the power electronics converter decouples the electrical interactions between generators and the power systems. This significantly reduces the system inertia as more and more SGs are replaced by CIGs, imposing a great challenge for maintaining system stability. The inertia of an SG is defined as the ratio between its kinetic energy and its rated power [14]; therefore, power system inertia is inherently provided by generators and turbines, which have kinetic energy stored in their rotating rotor masses [5]. Inertia helps counter frequency variations from the nominal value in the presence of power and generation before the primary response is activated. With increasing penetrations of CIGs, the total inertia of the power system, which is defined as the weighted sum of SGs' inertia, is gradually decreasing. This is because CIGs do not inherently provide inertia, i.e., PV systems, or because its inertia is isolated from the power systems due to the power converters [6]-[7], i.e., wind power. Fig. 1 shows the scenario where the replacement of traditional SGs with CIGs leads to reduced system inertia. The reduced inertia might lead to the unintended triggering of over-/underfrequency relays, load-shedding, and special protection schemes [8]-[9]. Indeed, because of the reduced system inertia, the rate of change of frequency (ROCOF) can reach unacceptable levels and might lead to cascading failures and blackouts (Australia, 2016; and the United Kingdom, 2019 [10]-[11]) [12].

To address these issues caused by low inertia, an accurate estimation of inertia is needed. Because of the intermittent nature of CIGs and loads, SGs might be switched on and off more frequently, yielding time-varying power system inertia [13]. With the development of wide-area measurement systems [14], the continuous awareness of power system inertia becomes a reality. In addition to inertia estimation, another challenge is how to quantify the virtual inertia from some CIGs. In CIGs, there are various types of energy storage systems,

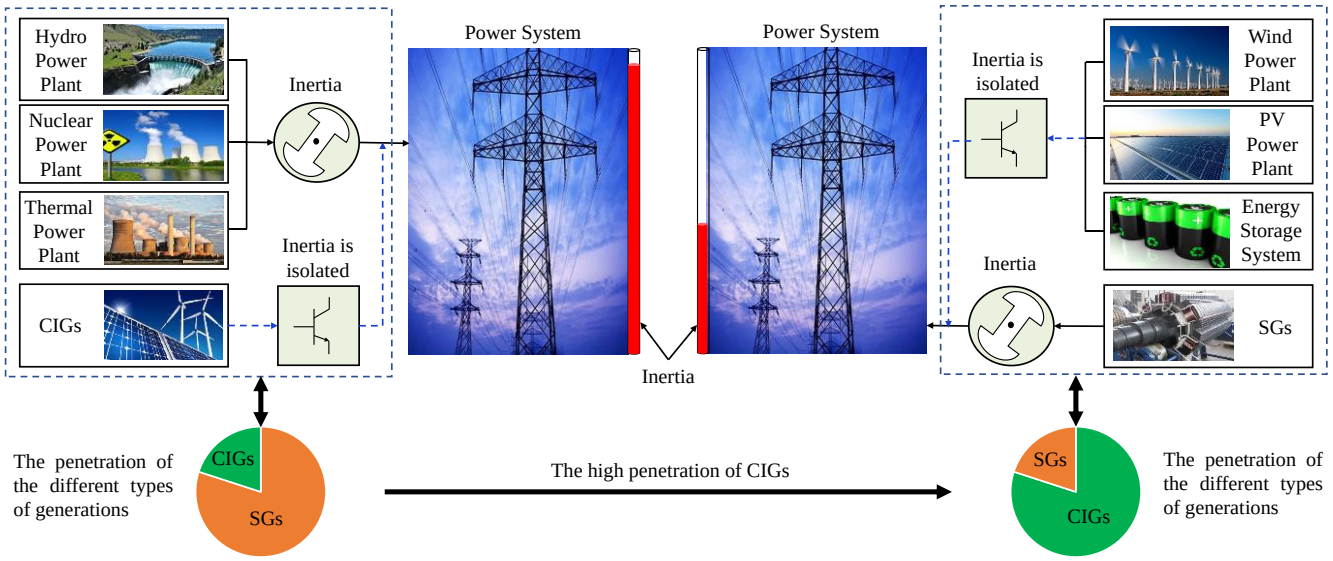

Fig. 1. Illustration of the reduced inertia in a power system with a high penetration of CIGs

including flywheels, capacitors, and batteries [5]. Because power converters are fast and allow CIGs to act more quickly than SGs [6], these types of energy storage systems can be used for frequency support via converter-based control—namely, virtual inertia emulation (VIE). The virtual inertia offered by the control of CIGs can be used to increase the inertial response of power systems [15]. The placement of virtual inertia in the power system also plays an important role in regulating the frequency response [16]. This calls for the development of new frameworks and methods to quantify virtual inertia from CIGs.

This paper aims to provide a comprehensive understanding of both rotating inertia and virtual inertia from CIGs and to review the corresponding estimation techniques. The contributions are summarized as follows:

- A comprehensive review of inertia estimation techniques is provided for SGs, including the model-based and measurement-based approaches. Different from [17] that categorizes inertia estimation approaches based on time horizon, this paper classifies the inertia estimation methods according to the types of modeling and the scale of disturbance. The advantages and disadvantages of different methods are also carefully discussed, and potential directions for improvements are offered.
- This is the first attempt to propose new potential algorithms for the estimation of the inertia from different VIE-based CIGs according to their various control characteristics. It allows us to quantitatively assess the contributions of CIGs and help predict future needs.
- New insights for future work on quantifying power system inertia considering CIGs and their potential applications are extensively discussed to shed light on developing new monitoring and control tools for the secure and reliable integration of more CIGs.

The rest of the paper is organized as follows. Section II shows the definitions of power system inertia, followed by a summary of different inertia estimation approaches in Section III. Section IV shows a new framework for the virtual inertia estimation of CIGs. Finally, Section V presents the conclusion and future work.

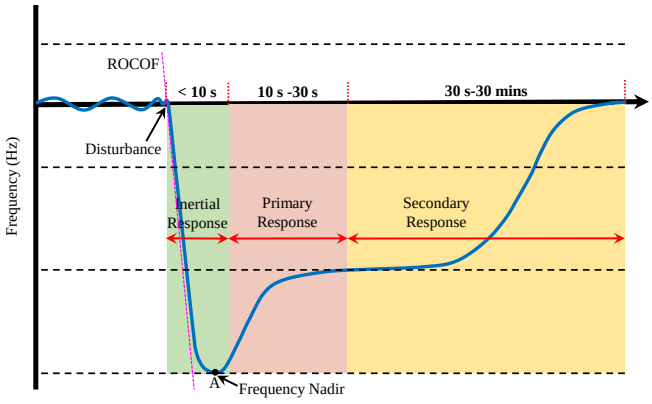

Fig. 2. Frequency responses with different timescales in a power system.

II. Definition of Power System Inertia

Generally, inertia is defined as the resistance to the change in the speed of the rotating masses in the SG-dominated system. By contrast, since CIGs generally provide virtual inertia via appropriate control, the inertia from CIGs needs to be carefully defined.

A. Frequency Response and Inertia Constant

During the imbalance between generation and demand, frequency responses with different timescales are involved in the power system, see Fig. 2 [18]. After a disturbance, e.g., a generation outage, the inertial response (generally less than 10 s) takes place. During the inertial response, the kinetic energy stored in the SGs is released to reduce the power generation loss so that the frequency nadir, can be reduced and the ROCOF is decreased [19]. Note that the frequency nadir is defined as the minimum value of frequency reached during the transient period. The primary response (generally 10 s–30 s) using the speed-governor control is activated to further reduce the frequency deviation. Finally, the secondary response, with automatic generation control (AGC), takes place within minutes to restore the frequency to the nominal level [8],[20].

In inertial response, rotating inertia mainly comes from generators and turbines in SGs [21]. Once a disturbance occurs, the unbalanced torque is applied to the rotors of the SGs, which causes an acceleration or deceleration of the SGs; thus, in a power system with N_{SG} SGs, the swing equation of the *i*-th SG can be formulated as [22]:

$$2H_{SG,i}\frac{d\Delta\omega_{g,i}}{dt}=\Delta P_{m,i}-\Delta P_{e,i}-D_i\Delta\omega_{g,i} \tag{1}$$

where $\Delta\omega_{g,i}$, D_i, $\Delta P_{m,i}$, and $\Delta P_{e,i}$ are the deviation of the rotor speed, the damping factor, the mechanical power, and the electrical power of the *i*-th SG, respectively. $H_{SG,i}=\frac{1}{2}J_i\omega_{m0}^2\Big/S_{B,i}$ is called the inertia constant, which is defined as the ratio between the kinetic energy and the rated power of the *i*-th SG, where J_i, $S_{B,i}$ are the moment of inertia and the rated power of the *i*-th SG, respectively; and ω_{m0} is the rated rotor speed. Depending on the types of SGs (i.e., hydro, nuclear and thermal, etc.), the rotational inertia constant ranges from 1.75 s to approximately 10 s, as shown in Table I [23]. Generally, with a given type of SGs, the larger the rated power, the larger the rotational inertia constant is. The right side of Eq. (1) represents the power imbalance caused by the disturbance. It can be concluded that small inertia leads to a large change rate of the rotor speed when the power unbalance is large.

TABLE I
The Inertia Constant of Different Types of Power Plants

Power plant type	Inertia Constant (s)
Hydro	1.75 ~ 4.75
Nuclear	4
Thermal	2 ~ 10

In the literature, the power system center of inertia frequency $\omega_{sys} = \sum_{i=1}^{N_{SG}} H_{SG,i}\omega_{g,i} \Big/ \sum_{i=1}^{N_{SG}} H_{SG,i}$ can be taken as a global parameter for a region so that all SGs can be aggregated into one equivalent unit. Then, Eq. (1) is rewritten as:

$$2H_{sys}\frac{d\Delta\omega_{sys}}{dt} = \Delta P_m - \Delta P_e - D_{sys}\Delta\omega_{sys} \tag{2}$$

where ΔP_m and ΔP_e are the total mechanical power change and the total electrical power deviation of the whole power system, respectively; D_{sys} is the system damping factor and H_{sys} is the rotational inertia constant of the regional system and can be calculated via:

$$H_{sys} = \frac{\sum_{i}^{N_{SG}} H_{SG,i}S_{B,i}}{\sum_{i=1}^{N_{SG}} S_{B,i}} \tag{3}$$

From Eq. (2), it can be found that the inertia constant shows the resistance to the change in rotor speed by exchange active power with the power system. With high penetrations of CIGs, the definition of inertia needs to be changed considering the different power control methods of CIGs.

B. Inertia Considering CIGs

In power converter-dominated power systems, a large number of SGs are replaced by CIGs; however, CIGs are initially inertia-free because of their operational characteristics. Among these CIGs, wind, and PV generations are the most promising sources [24]; however, the maximum power point tracking control is used [25]-[26], which prevents wind and PV generation from providing active power support to counteract the frequency change [27]. Note that doubly-fed induction generators (DFIGs) have been widely applied due to their variable speed constant frequency operation capacity [28]. Though DFIGs have rotating inertia from wind turbines, that is isolated by power converters.

Although CIGs typically do not have three frequency response processes like SGs, including inertia response, primary frequency response via speed-governor control, and AGC, a virtual inertia response can be conducted through the control of power converters [29]. Therefore, the non-rotating inertia can be obtained from CIGs through suitable control methods. Assuming there are N_{CIG} CIG units with virtual inertia control in the power system, the definition of inertia considering CIGs can be obtained as [23], [30]:

$$H_{eq} = \frac{\overbrace{\sum_{i=1}^{N_{SG}} H_{SG,i}S_{B,i}}^{(SGs)} + \overbrace{\sum_{j=1}^{N_{CIG}} H_{CIG,j}S_{B,j}}^{(CIGs)}}{\sum_{i=1}^{N_{SG}} S_{B,i} + \sum_{j=1}^{N_{CIG}} S_{B,j}} \tag{4}$$

leading to a more general swing equation as:

$$2H_{eq}\frac{d\Delta\omega_{eq}}{dt} = \Delta P_m - \Delta P_e - D_{eq}\Delta\omega_{eq} \tag{5}$$

where $\Delta\omega_{eq}$ is the deviation of the equivalent frequency; D_{eq} is the equivalent damping factor; H_{eq} is the equivalent inertia; $H_{CIG,j}$ is the virtual inertia of the *j*-th CIG; and $S_{B,j}$ denotes the rated power of the *j*-th CIG. Inertia in Eq. (5) consists of two parts: 1) the rotating inertia from SGs and 2) the virtual inertia from CIGs. Note that $H_{CIG,j}$ is generally unknown and time-varying because it depends on the operating states and control methods for CIGs.

III. Classification of Inertia Estimation Approaches

In a conventional power system, the inertia constant is selected as the valuable reference for frequency control and protection [22]; however, the inertia constant becomes complex and time-varying because of the integration of CIGs, causing difficulties for operators to track it. Inertia estimation approaches can be divided into two main categories: 1) model-based and 2) measurement-based approaches; see Fig. 3. They are discussed from Section III-A to Section III-B.

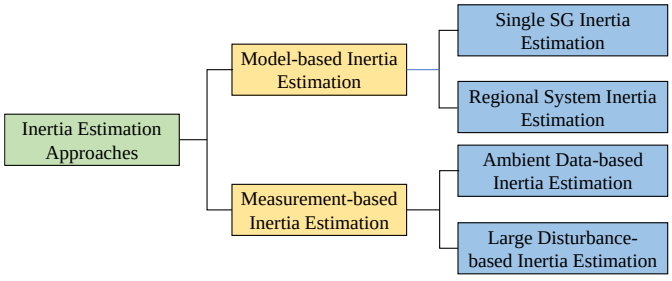

Fig. 3. Classification of inertia estimation approaches.

A. Model-Based Inertia Estimation

The model-based inertia estimation relies on a dynamic model of SGs, which can be written as [31]:

$$\begin{cases} \dot{\boldsymbol{x}} = \boldsymbol{f}(\boldsymbol{x},\boldsymbol{u},\boldsymbol{\theta}) \\ \boldsymbol{y} = \boldsymbol{h}(\boldsymbol{x},\boldsymbol{\theta}) \end{cases} \tag{6}$$

where, $\boldsymbol{x}$, $\boldsymbol{y}$, and $\boldsymbol{\theta}$ are the state variables, algebraic variables, and the parameters of the SG, respectively; $\boldsymbol{f}$ and $\boldsymbol{h}$ are nonlinear vector-valued functions; and $\boldsymbol{u}$ denotes the vector

of control inputs. Note that inertia constant is included in the parameters $\boldsymbol{\theta}$, and to estimate it, the objective function is [32]:

$$\min \quad J(\boldsymbol{\theta}) = \frac{1}{2}\int_0^{T_0} \left\| \boldsymbol{y} - \hat{\boldsymbol{y}} \right\| dt \tag{7}$$

where $\hat{\boldsymbol{y}}$ is the calculated values based on estimated $\boldsymbol{\theta}$, and T_0 is the length of the dynamic trajectories of $\hat{\boldsymbol{y}}$ and $\boldsymbol{y}$.

The induction motor also provides inertia after a disturbance; however, there are few works in the literature on that. These are estimated using experiments [33]-[34] or a parameter identification approach similar to Eq. (7) [35]. This subsection illustrates only model-based inertia estimation for SGs.

(1) ***Single SG inertia estimation***: In [36], the extended Kalman filter is used to identify the inertia constant using the simplified generator model. The least-squares [37]-[38], optimization technique [39], and various Kalman filter methods [40]-[42] are also applied to identify the inertia constant in an SG subject to large disturbances. Following their work, an inertia estimation technique based on a Kalman filter for SGs with different controllers is proposed in [43]-[45]; however, they are limited to the reduced-order generator model. Extensions of them to the detailed model of SGs are done in [46]-[48], where both the balanced [46]-[47] and unbalanced operation conditions [48] are investigated.

(2) ***Regional system inertia estimation***: To reduce the computational complexity of solving differential-algebraic equations (DAEs) with many SGs, the dynamic equivalent of SGs that have coherency is developed [49]; see Fig. 4. In other words, those SGs are taken as an equivalent SG, and this allows us to estimate the equivalent inertia of a regional system. In [50]-[51], the dynamic equivalent of a generator and a load in parallel are constructed, and their equivalent parameters are identified through the genetic algorithm. Along the same lines, an analytical dynamic equivalencing framework is developed in [52] for two-area and three-area power systems, but it is not suitable for multiarea power systems with more than three areas. To address that, the dynamic equivalent of multiarea power systems is achieved in [53]-[54] by decoupling the estimation process into two stages: the mechanical parameter (such as the inertia constant) estimation is followed by the electrical parameter (such as impedance) estimation, whereas [55]-[56] establish the dynamic equivalent of each area by obtaining the mathematical relationship between the dynamic parameters (inertia constant and damping factor) and the electromechanical oscillation parameters extracted from phasor measurement unit (PMU) measurements. Further, the mixed external equivalent (SGs + loads) of an area is proposed in [57] by merging the unknown parameters of different components into DAEs.

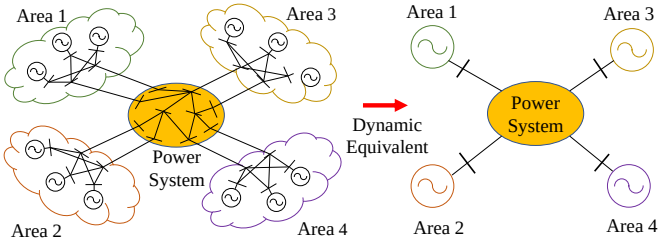

Fig. 4. Illustration of the dynamic equivalent of a regional power system

The model-based methods have been extensively used for the inertia estimation of SGs, but the estimation accuracy depends on the model accuracy. Specifically, the equivalent inertia estimation of a regional power system relies on a suitable area division based on SG coherency. Also, they might not be able to estimate the virtual inertia provided by CIGs if the dynamics of CIGs are not emulated by the swing equations or if the control schemes are unknown. Note that model-based virtual inertia estimation of non-synchronous devices is performed in [58]-[59] with frequency divider formula [60], which needs only the network admittance matrix and internal reactance obtained by Thevenin equivalent. However, the transmission line and the transformer parameters are always affected by uncertainties, leading to an imprecise network admittance matrix. Furthermore, the internal reactance of CIGs is difficult to identify. This motivates the measurement-based methods.

B. Measurement-Based Inertia Estimation

The development of wide-area measurement systems leveraging Global Positioning Systems provides massive real-time measurements to enable wide-area monitoring and control applications [61]; thus, different inertia estimation strategies using PMU measurements have been proposed. In this section, these strategies are discussed and categorized from the perspective of using large disturbances or ambient data.

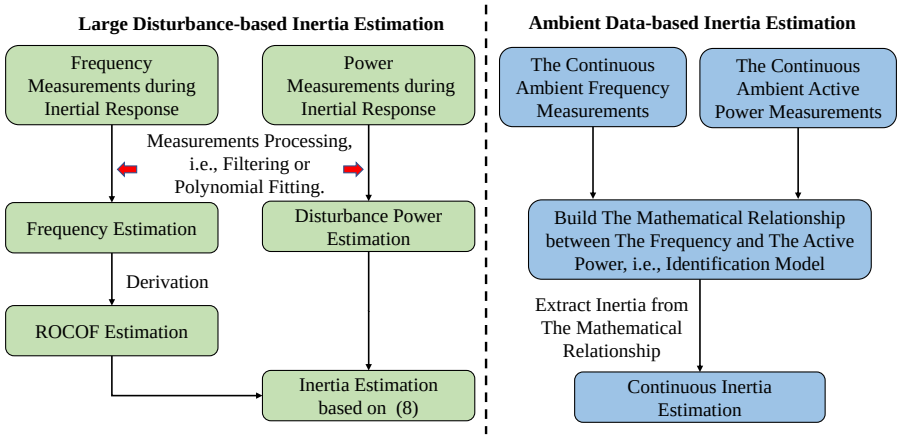

Fig. 5. The general process for measurement-based inertia estimation.

1) Large Disturbance-Based Inertia Estimation

When power systems are subject to a large disturbance, the power imbalance in the inertial response stage is caused mainly by the electrical power deviation. This is because the generator governor has a longer response time than the inertial response. Subsequently, the mechanical power maintains a steady state or presents only an extremely small change in the inertial process [62]; therefore, to illustrate the frequency dynamics during the inertial response, Eq. (5) can be rewritten as:

$$2H_{eq}\frac{d\Delta\omega_{eq}}{dt} = -\Delta P_e \tag{8}$$

Note that the damping term is too small to be neglected when performing inertia estimation.

After a disturbance, some loads are frequency-dependent and voltage-dependent. This can affect the electrical power deviation, ΔP_e . Further, the size of the disturbance is a critical factor in affecting the electrical power deviation; thus, (8) is further converted to be [63]:

$$2H_{eq}\frac{d\Delta\omega_{eq}}{dt} = -(\Delta P_L + \Delta P_{dist}) \tag{9}$$

where $\Delta P_e = \Delta P_L + \Delta P_{dist}$ and ΔP_L represents the power variations of frequency-independent and voltage-independent loads. ΔP_{dist} is the size of the disturbance. Generally, in some cases—such as generator tripping, load rejection, and outage of a feeder or a DC-link connection—the size of the disturbance can be known. From Eq. (9), the accurate inertia estimation is mainly determined by the change rate of rotor speed and the electrical power deviation. Because the change rate of the rotor speed is unavailable in PMU measurements, the change rate of the generator terminal frequency—namely, the ROCOF—is used as a proxy. As a result, Eq. (8) is reformulated into $2H_{eq}\, d\Delta f_b/dt = -\Delta P_e$, where f_b is the generator terminal frequency. The overall process of large disturbance-based inertia estimation is shown on the left-hand side of Fig. 5.

(1) **ROCOF estimation**: If ROCOF is directly calculated by the differential of frequency measurements, it is prone to noise [64]. Therefore, alternative approaches are developed to eliminate noise and sharp transient-type changes in frequency measurements, yielding a more accurate estimation of ROCOF. A fifth-order polynomial for the frequency response before the ROCOF estimation is first proposed in [65], whereas [66] assumes the average system frequency $\tilde{f}(t)$ to be:

$$\tilde{f}(t) = k[1 + \alpha e^{-\beta\omega_1 t}\sin(\omega_2 t + \phi)] \tag{10}$$

where k , α , β , ω_1 , ω_2 , ϕ are the unknown parameters. The curve fitting [65]-[66] is performed using linear least-squares so that the impacts of transients and noise on the ROCOF estimation can be minimized; however, the ROCOF estimation is affected by the frequency measurements beyond the inertial response. Thus, a 500-ms sliding window is employed to sample measurements in the time interval of 1 s after the disturbance [67], which avoids the impacts of the primary response. Following that work, [68] proposes a variable-order polynomial fitting for frequency response so that the adaptivity of the curve fitting is increased. Further, a linear frequency model is established to reduce the complexity of the curve-fitting model [69], which allows for the use of a short data window for ROCOF estimation. In [70], an equivalent second-order homogeneous differential equation is built to reconstruct the frequency deviation signal in a bus with the equivalent modes, avoiding the selection of a time window and the impacts of a phase step error. There is another kind of ROCOF estimation method based on the low-pass filter. To eliminate the transient sharp change and noise in frequency signals, a low-pass filter is employed to isolate the dominant system inertial frequency response [18], [73]-[74], whereas [75] combines the low-pass filter with the curve fitting to make a trade-off between the removal of oscillations and the minimum deviation between the original signals and the processed signals; however, the low-pass filter introduces a time delay.

(2) **Disturbance power estimation**: The accuracy in power imbalance estimation also has huge impacts on the inertia estimation. In [76], the electrical power deviation at the instant after the disturbance is used to perform the inertia estimation of a single SG. To eliminate the impacts of noise, [73] and [74] employ two sliding data windows to filter the noise in the active power before and after the disturbance, respectively. A fifth-order polynomial is chosen to perform active power trajectory fitting at all generator terminals [68]; however, they assume that the electrical power can be measured at every terminal bus, which might not be practical. Thus, in [77], the inertia of the

TABLE II
COMPARISONS BETWEEN DIFFERENT METHODS FOR INERTIA ESTIMATION

Estimation Category	Estimation Window	Advantages	Disadvantages
Model-based inertia estimation	Seconds to tens of seconds	• Explicitly mathematical expression	• Dependent on modeling and large disturbance • Limited to the inertia estimation of SGs • Suffering from parameter uncertainties
Measurement-based inertia estimation using large disturbance data	Seconds	• Model-free • Fast	• Difficult to estimate ROCOF • The boundary between inertial response and primary response is unclear • Dependent on large disturbance • Using generator terminal bus frequency as a proxy for generator rotor speed
Measurement-based inertia estimation using ambient data	Minutes	• Model-free • Continuous tracking of inertia	• Using generator terminal bus frequency as a proxy for generator rotor speed • Vulnerable to measurement noise.

local area power system is obtained by applying a boundary power deviation to Eq. (8), relaxing the assumption that the electrical power can be measured at each bus. Further, in [78], the change of the aggregated load and the size of the disturbance are taken to represent the electrical power deviation, where the change in the aggregated load is depicted according to the overall voltage profile, V_s , of the power system, see Eq. (11).

$$\Delta P_L = P_{L0}(V_s - 1) \tag{11}$$

where P_{L0} is the total load before the disturbance. This work is extended considering a small power change caused by the frequency dynamics associated with the governors [79]. Because the aggregation of the components is performed, it can calculate only the effective inertia of the power system.

Once the disturbance happens, inertia can be estimated in seconds. But because the large disturbance-based inertia estimation relies on the occurrence of transient events, it might not be implemented to achieve continuous awareness of the inertia because the transient events are infrequent. Further, during the disturbance, the inertial response is difficult to distinguish from the primary response, especially when the time delay needs to be included in the virtual inertial control by the CIGs. The next section discusses ambient data-based inertia estimation.

2) Ambient Data-Based Inertia Estimation

Ambient data obtained from PMUs reflect the stochastic system response time series caused by random load and renewable energy changes [80]-[81]. The ambient data-based methods are developed for system inertia estimation as well as bus inertia estimation. In [82], the equivalent inertia estimation using the Markov Gaussian method is proposed, where the model is trained to extract the hidden relationship between the average frequency variations and the system inertia. Along this line, [83] uses ambient frequency deviation and active power deviation to build a multi-input–multi-output ARMAX model, which represents a combined model of the inertial response and the primary response. This allows for estimating the system inertia from the impulse response of the model. A closed-loop identification model shown in [84] is proposed to perform online system inertia estimation, but it requires a well-designed probing signal. The system inertia estimation is denoted as a regression model in [85] and can be solved by dynamic regressor extension and mixing. To estimate the inertia of the regional power system, [86] develops an online estimation of the effective inertia in each area by adopting the values of inter-area oscillation modes calculated from ambient data. Further, a dynamic model for each generator is identified in [87], which relates the active power and bus frequency. Then, the inertia of each generator is extracted by applying a unit step signal to the identified model. This work is later extended to the bus inertia distribution estimation using the mathematical relationship between the bus frequency and the generator rotor frequency [88].

The overall process of ambient data-based inertia estimation is shown on the right-hand side of Fig. 5. Compared with other methods, the ambient data-based approaches can perform continuous estimation of inertia; however, minutes of data are needed to identify the dynamic model. The comparisons among different methods for inertia estimation are further summarized in Table II.

3) Discussions of Challenges and Potential Solutions

Although measurement-based inertia estimation methods are suitable for real-time inertia calculation, there is a key challenge limiting their application. Both are essentially based on the swing equation, so the rotor speed of SGs must be known; however, the rotor speed is approximated by the corresponding generator terminal bus frequency in the existing literature—this is because the measurements of the generators' rotor speed and angle are not available [89]. Indeed, this approximation could lead to large errors, which is explained next.

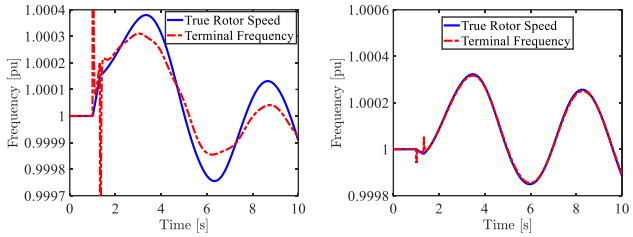

(a) (b)

Fig. 6. Terminal bus frequency under different fault conditions: (a) $x'_d = 0.12$ pu and the fault line is 9-39; (b) $x'_d = 0.006$ pu and the fault line is 9-39.

(1) **Terminal frequency errors in the presence of large disturbances**. The generator's rotor speed is one of the true state variables that govern the DAEs of power systems, so it does not change instantly; however, spikes caused by a disturbance—e.g., a short-circuit fault—lie in the generator terminal bus frequency because it is an algebraic variable derived by taking the derivative of the phase angle with respect to time. This leads to a large error in the ROCOF calculation. Take the simulation results from the IEEE 39-bus power system as an example [90]. When a three-phase short circuit applied on Bus 9 clears by removing line 9-39 after 0.33 second, Fig. 6(a) shows that there are spikes in the calculated terminal bus frequency. This greatly affects the accuracy of the ROCOF calculation.

(2) **Deviation between the rotor speed and the generator terminal frequency.** According to the frequency divider formula [60], the relationship between the rotor speed and the generator terminal bus frequency can be described by:

$$\Delta\omega_g = \Delta f_b - x_{eq}\frac{dP_e}{dt} \tag{12}$$

where x_{eq} is the equivalent generator internal reactance. For example, for the round rotor generator, the d-axis transient reactance, x'_d , equals x_{eq} . Δf_b is the generator terminal bus frequency. According to Eq. (12), the larger the value of x_{eq} , the greater the difference between the rotor speed and the terminal bus frequency; see Fig. 6(a) and Fig. 6(b). Therefore, to eliminate the terminal frequency error, an alternative way is to directly estimate the rotor speed.

(3) **The impacts of measurement issues on power imbalance calculation.** As illustrated in Section III-B, the influence of measurement noise on the power imbalance estimation can be mitigated; however, there can be bad data and missing data, which could significantly reduce the precision of the power imbalance determination. Further, not all buses are equipped with PMUs, so regional system inertia estimation can be challenging. More research is needed to estimate the power imbalance when estimating the regional system inertia.

IV. Virtual Inertia Estimation

To mitigate frequency instability issues caused by the integration of CIGs, virtual inertia emulation (VIE) is widely studied to increase the inertia level in the power system [91]. VIE can be implemented via appropriate control strategies on converters. To quantify the entire inertia of power systems, VIE must be considered. However, there is limited work on virtual inertia estimation. Therefore, this section focuses on defining VIE and proposes potential methods for its quantification.

A. Brief Summary of VIE Methods

1) Direct Inertial Control-Based VIE

Synthetic inertia - (SIC-) based VIE is performed based on the ROCOF and frequency deviation to realize the dynamic frequency regulation [92]. Its main control strategy is based on Eq. (13):

$$\begin{aligned} P_c &= P_{ref} + \Delta P \\ &= P_{ref} - K_d \frac{df_b}{dt} - K_e(f_b - f_n) \end{aligned} \tag{13}$$

where P_{ref} is the reference of active power; ΔP is the change of active power; and P_c is the active power controlled by the converter. The terminal frequency, f_b, can be obtained from the terminal voltage angle using a phase-locked loop (PLL) [93], whereas f_n is the nominal frequency in the power system. K_d is the coefficient of the ROCOF loop, and K_e is the coefficient of the droop loop. The control scheme is illustrated in Fig. 7, where $\tilde{\boldsymbol{V}}$ is the terminal voltage phasor.

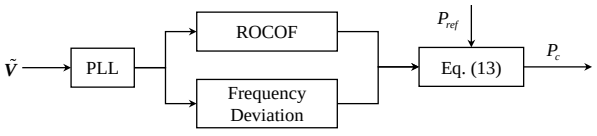

Fig. 7. The control scheme of SIC-based VIE.

SIC-based VIE has been widely used in CIG applications. **For wind generations**, the coefficients K_d and K_e are tuned according to the minimum frequency nadir and the maximum ROCOF in [94], whereas [95] calculates them from the viewpoint of protecting the wind turbine rotor from stalling. Further, because the coefficients are constant and thus lack adaptability during the inertia contribution, the dynamic adaptive coefficient K_e -based inertial control is presented in [96]-[97]. In [96], K_e is obtained with a function of ROCOF so that the ROCOF loop can be merged into the droop loop to overcome the drawbacks in each loop. K_e in [97] is calculated using the power margin of the wind turbine generator to avoid over-deceleration. **For PV generation**, the SIC-based VIE is developed mainly by using energy storage or the energy from the DC-link capacitor. In [98], the energy storage is used to provide SIC-based VIE in PV systems, and the size of the energy storage is also determined considering the maximum allowed frequency deviation during the disturbance. In addition to the energy storage, the energy from the PV DC-link capacitor is further used to provide inertia support in [99], though this requires PV to work below the maximum power point mode. Because energy storage is expensive, especially for small productions, the potential energy from the DC-link capacitor is extracted to perform the inertia emulation to reduce the cost and to improve the performance of VIE [100]. The DC-link capacitor and PV systems with suboptimal operation can also be coordinated for dynamic frequency regulation [101]. In [102], only PV systems are employed to provide SIC-based VIE, but PV systems should maintain sufficient power reserve for that.

2) Virtual Synchronous Generator-Based VIE

Virtual synchronous generator- (VSG-) based VIE emulates the SG model in the control algorithm of the coupling converter so that CIGs behave like an electrical rotating machine providing virtual inertia. VSG-based VIE can be achieved by controlling the charging or discharging of the storage devices or by acquiring excessive energy from inertia-free CIGs, such as PV and wind generation, both type 3 and 4. Generally, this control strategy can be divided into 1) grid-forming control and 2) grid-following control [103], but the core component of the VSG-based VIE is the swing equation with the damping term, i.e., [104]:

$$P_{in} - P_{out} = 2H_{VSG} \frac{d\omega_{VSG}}{dt} + D_{VSG}\Delta\omega_{VSG} \tag{14}$$

where H_{VSG} is the virtual inertia; D_{VSG} is the damping factor; ω_{VSG} is the virtual rotor speed; P_{in} is the virtual shaft power; and P_{out} is the measured power output. Thus, the inertial characteristic of an SG is mimicked by the VSG.

Increasing numbers of CIGs are being connected to power systems, leading to a significant reduction in inertia. A VSG is a promising approach to providing VIE to help regulate frequency [105]-[106]. Because the simplified model of an SG is embedded in converters, a VSG has the advantage of quickly adjusting the VIE parameters to obtain better performance on the frequency response; thus, variable inertia can be achieved during operations. Motivated by that, an alternating inertia control scheme is designed in [107], where the switch between the large inertia constant and the small inertia constant is defined according to the relative virtual rotor speed. The damping and stability effects of the alternating inertia control scheme are further clarified in [108] with the transient energy function analysis. Note that the inertia in these works is assumed to be constant during each time switch interval. The authors in [109] and [110] develop the self-adaptive VIE and

virtual damping control together to mitigate ROCOF and the frequency deviation while reducing the oscillations.

3) Limitations of VIE Model

VIE model can behave like input-output dynamics of SGs, so it is compatible with the legacy of power system. Though emulating inertial response is advocated for CIGs to support frequency, there are some limitations due to the limited capacity of converters [8]. On one hand, there are actuation delays, which can be up to 100 ms introduced by signal processing (such as PLL) and control loops in converters; on the other hand, VIE control is subject to current limitation during post-contingency dynamics due to the limited current constraints of converters. Thus, VIE model has limited capability of imitating the inertial response of SGs and the complexity of the model is further increased. This calls for the development of new inertia estimation techniques.

B. Inertia Estimation for CIGs with VIE Control

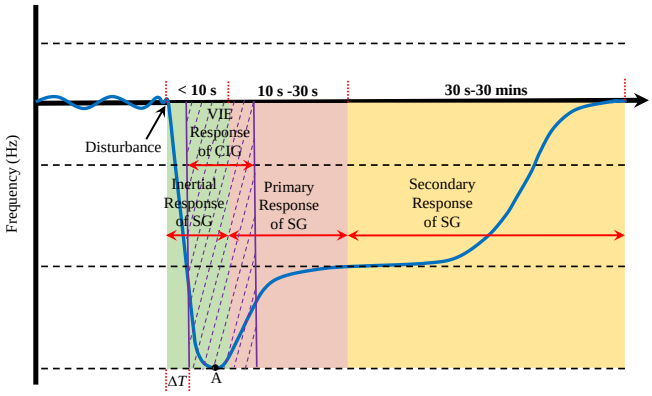

Fig. 8. VIE response of CIGs during frequency response.

Different from SGs, the CIGs can leverage the PLL and inner-loop current control to achieve fast frequency control; however, these control schemes usually introduce a time delay, i.e., PLL, which means that the VIE control is not as quick as the physical rotating inertial response. Assuming that the time delay in the VIE control is ΔT and that its valid response is activated during the time shown by the dotted line in Fig. 8, it was found that some overlapping might exist in the primary response of SGs and the VIE response of CIGs. This results in challenges in inertia estimation, especially for regional systems with both SGs and CIGs. From Section IV-A, it is known that the time-varying VIE can be deployed for CIGs. To accurately quantify the available inertia, it is vital to extract the real-time inertia supplied from the CIGs themselves. The next subsection discusses the inertia estimation scheme for individual and aggregated CIGs.

1) Individual CIG Inertia Estimation

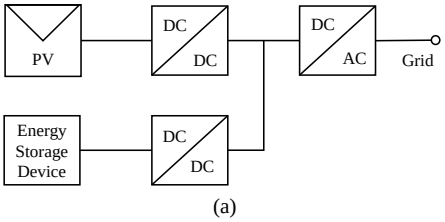

(a)

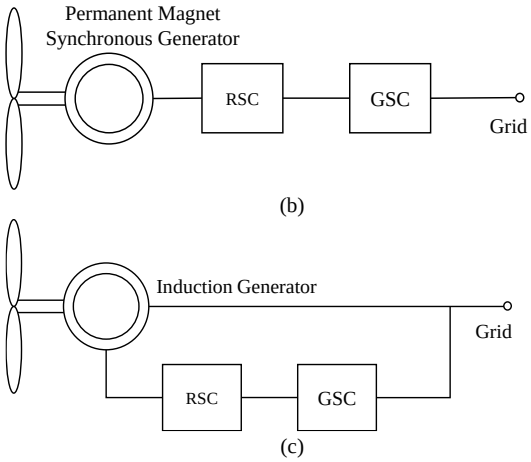

(b)

(c)

Fig. 9. Block diagram for different types of CIGs: (a) PV and energy storage system [112]; (b) Full converter wind turbine (Type-4) [113]; (c) Doubly-fed induction generator (Type-3) [28].

TABLE III
PROPOSED APPROACHES FOR INERTIA ESTIMATION OF CIGS

The type of CIG inertia estimation	The type of CIG VIE control	The key requirements for inertia estimation
Individual CIG inertia estimation	SIC-based VIE of PV system and FCWT	Tracking the time-varying coefficients
	All types of VIE control of DFIG	Estimating rotor speed via DSE
	VSG-based VIE of PV system and FCWT	Estimating virtual rotor speed via DSE
Aggregated CIG inertia estimation	All types of VIE control for CIGs	Using total regional system inertia to subtract the inertia from other devices

CIGs are typically integrated into power systems using converters; see Fig. 9. A PV system can be equipped with an energy storage device or operated in non-maximum power point mode to provide inertia. For the energy storage device, its capacity and state of charge (SOC) determine the available energy, which further limits the amount of virtual inertia that can be emulated via controls; the DC-DC converter is a boost chopper, which regulates the charging and discharge rate of energy storage device [112]. This also posts some limits on the virtual inertia emulation control. In contrast, the full-converter wind turbine (FCWT) [113]and DFIG perform VIE by controlling the grid-side converter and rotor-side converter by releasing the kinetic energy stored in the rotor. Fig. 8 shows that PV systems and FCWTs are completely decoupled from the power system, but DFIGs are not; thus, with different types of CIGs and VIE controls, it is important to develop various approaches for inertia tracking, which are summarized in Table III.

Since DFIGs are still directly connected to the power system, their inertia can be estimated by obtaining rotor speed no matter which type of the VIE control is used; however, works on the rotor speed estimation of DFIGs are still limited because of their increased complexity compared to SGs [114]. Though the extended Kalman filter, the unscented Kalman filter, and the unscented particle filter-based dynamic state estimation (DSE) have been developed for DFIG rotor speed estimation [114]-[117], the estimation accuracy needs to be further improved. VIE control should be also included for the DSE of DFIG. On the other hand, the DIFG model complexity might be very high

and is subject to various sources of uncertainty, a reduced-order model might be developed for rotor speed estimation without a loss of accuracy. Robust DSE is needed to be able to filter out the noise and suppress model uncertainties.

Compared with DFIGs, PV systems and FCWTs are decoupled from the grid, so different methods are needed for inertia estimation. With SIC-based VIE, the core step is to obtain an accurate terminal frequency estimation so that the coefficients of SIC-based VIE can be calculated. But how to track the time-varying coefficients is still an open problem. With VSG-based VIE, this means that PV systems and FCWTs behave like SGs, so the virtual rotor speed in VSGs can be used to conduct inertia estimation. This requires an accurate estimation of the virtual rotor speed from measurements. DSE-based approaches can be good candidates for that. Other signal-processing-based parameter identification methods can also be developed.

2) Aggregated CIG Inertia Estimation

Individual inertia estimation model can provide a comprehensive insight for the temporal-spatial inertia distribution. However, the individual inertia estimation may not be very accurate or available due to the lack of sufficient number of measurements or inaccurate model. For some applications, we may be interested in the inertia available from the aggregated CIGs at a regional level. Performing the inertia estimation for each CIG and adding them together can be challenging and time-consuming.

To address this issue, an alternative way to achieve this is to obtain the aggregated inertia from other devices, such as SGs and induction motors using a limited number of measurements. Once the inertia from these devices is determined and the regional system inertia is estimated via the boundary information—such as the boundary power and the boundary frequency—the inertia provided by the aggregated CIGs can be obtained by subtracting the inertia of other devices from that of the regional system. On the other hand, for a large wind or PV power plant with many small generators, an equivalent model that captures the swing equation responses can be inferred, and advanced system identification approaches should be proposed to estimate the aggregated inertia for them. Note that for a large wind or PV power plant, not all small generators are online or functioning properly, leading to time-varying aggregated inertia. This calls for the development of recursive estimation approaches to track time-varying aggregated inertia, such as recursive least squares and Kalman filter-based DSE.

V. Conclusion and Future Work

This paper presents an overview of inertia definitions as well as the estimation methods for SGs and CIGs. The approaches in estimating SGs have been categorized into model-based and measurement-based methods. Individual-level and system-level inertia estimation is also discussed. The advantages and disadvantages of different categories of inertia estimation methods are highlighted. This paper also offers a unique potential framework to quantify and track virtual inertia from CIGs. This paper can serve as a guideline for researchers in the area of inertia estimation.

Although some progress has been obtained, there are many open problems, and some of them are discussed next:

- **Robust estimation of rotor speed and virtual internal frequency**: Among various inertia estimation methods, SG terminal frequency is usually used as a proxy of rotor speed. This can lead to large errors, as illustrated in Section III-C; thus, it is necessary to develop proper approaches for rotor speed estimation for SGs or virtual internal frequency for VIE-based CIGs. For SGs, the estimation for the rotor speed should reach an acceptable accuracy as soon as possible (i.e., 2–3 seconds) because the inertia estimation of SGs is affected by the vague boundary between the inertial response and the primary response. Using the ambient measurements, an alternative way to perform inertia estimation for SGs might be to reconstruct rotor speed and the active power, such as the Koopman operator approach [119], but measurement issues—i.e., noise and bad data—need to be carefully addressed. For VIE-based CIGs, the control details are usually not known in practice, so the virtual internal frequency estimation for the black box should be formulated. Advanced system identification approaches and DSE are needed. Machine learning-based methods might also be developed to identify the relationship between inertia response and measurements after disturbances [120]. Reduced-order models for CIGs can be good candidates that allow us to develop optimization- or DSE-based methods in estimating and tracking time-varying virtual inertia from CIGs. The impacts of different control strategies and operating conditions on CIGs' inertia should be carefully investigated.
- **Inertia estimation for CIGs using ambient measurements or local signal perturbations:** The ambient measurement or local signal perturbation-based inertia estimation is promising in quantifying the inertia in power systems, whereas other approaches heavily depend on the occurrence of large disturbances, and accurate and detailed models are needed. On one hand, the existing works require minutes of measurements to obtain an accurate estimation of inertia. Determining the trade-off between computational efficiency and accuracy needs to be addressed, i.e., the selection of appropriate measurement channels and time windows. The control setting points of CIGs can be changed strategically to produce perturb signals for inertia identification. The magnitudes, as well as the lengths of the perturbations, must be properly designed. CIGs have much faster response speeds than SGs. When quantifying the system inertia, how to effectively distinguish the responses from SGs and CIGs for proper inertia estimation would be important in achieving high accuracy. Advanced clustering or machine learning approaches can be developed to identify the essential patterns for SGs and CIGs so that inertia quantifications of them are not cross-affected.
- **Inertia estimation uncertainty quantification**: Because of the stochasticity and uncertain nature of CIGs, the inertia estimation outcomes also contain uncertainties. Providing confidence intervals for the estimated inertia would be essential to justify the estimation accuracy. Probabilistic estimation methods or variance-based analysis for an

estimator need to be developed so that the mean and its uncertainties can be derived.

- **Spatial-temporal inertia distribution analysis:** Because increasing numbers of CIGs are equipped with VIE controllers, the virtual inertia varies all the time. For instance, if a PV system or wind generator is equipped with adaptive VIE, the virtual inertia will change with the system operating conditions. Because generators that provide inertia are placed at different locations, inertia is also spatially distributed. In other words, inertia is featured with the spatial-temporal distribution characteristic. Existing works mainly focus on exploring the local or systematic inertia tracking, and more research is needed to investigate the spatial-temporal inertia distributions on each bus. Also, the relationship between the spatial-temporal bus inertia and the generator inertia needs to be better understood. This could be achieved via the frequency divider formula and electromechanical wave propagation theory [119]. This allows us to have both local and global views of frequency changes subject to disturbances, significantly enhancing the operator's situational awareness.
- **Inertia-based applications:** Inertia service is free in traditional SG-dominated power systems because SGs instantaneously respond to power imbalance. The replacement of SGs by CIGs significantly reduces the system inertia and the virtual inertia provided by CIGs may need incentives, e.g., adequately designed ancillary services so that enough virtual inertia from CIGs can be obtained. This calls for the development of inertia-constrained unit commitment, inertia-constrained optimal power flow for frequency stability assessment, and stability control by harvesting inertia contributions from CIGs. The availability of online system inertia also allows us to predict the frequency nadir, benefiting the power reserve planning and preventive control.

ACKNOWLEDGEMENTS

This work was authored in part by the National Renewable Energy Laboratory, operated by Alliance for Sustainable Energy, LLC, for the U.S. Department of Energy (DOE) under Contract No. DE-AC36-08GO28308. Funding provided by U.S. Department of Energy Office of Energy Efficiency and Renewable Energy Wind Energy Technology Office. The views expressed in the article do not necessarily represent the views of the DOE or the U.S. Government. The U.S. Government retains and the publisher, by accepting the article for publication, acknowledges that the U.S. Government retains a nonexclusive, paid-up, irrevocable, worldwide license, to publish or reproduce the published form of this work, or allow others to do so, for U.S. Government purposes.

REFERENCES

[1] N. Hatziargyriou *et al*., "Definition and classification of power system stability revisited & extended," *IEEE Trans. Power Syst.*, vol. 36, no. 4, pp. 3271-3281, Jul. 2021.

[2] WWEA, *Focus on renewable energy has to be core element of a strategy to restore and green the global economy*, 2020. [Online]. Available: https://wwindea.org/blog/2020/04/16/world-wind-capacity-at-650-gw/.

[3] PV-magazine, *World now has 583.5 GW of operational PV*, 2020. [Online]. Available: https://www.pv-magazine.com/2020/04/06/world-now-has-583-5-gw-of-operational-pv/.

[4] V. Vittal, J. D. McCalley and P. M. Anderson, *et al*., *Power system control and stability*. Hoboken, NJ, USA John: Wiley & Sons, 2019, pp. 13-16.

[5] M. H. Othman, H. Mokhlis and M. Mubin, *et al*., "Progress in control and coordination of energy storage system-based VSG: a review," *IET Renewable Power Generation*, vol. 14, no. 2, pp.177-187, Feb. 2019.

[6] M. F. M. Arani and E. F. El-Saadany, "Implementing virtual inertia in DFIG-based wind power generation," *IEEE Trans. Power Syst.*, vol. 28, no. 2, pp. 1373-1384, May. 2013.

[7] D. Wilson *et al*., "Measuring effective area inertia to determine fast-acting frequency response requirements," *International Journal of Electrical Power & Energy Systems*, vol. 113, pp. 1-8, Dec. 2019.

[8] F. Milano, F. Dörfler and G. Hug *et al*., "Foundations and challenges of low-inertia systems," in *2018 Power Systems Computation Conference (PSCC)*, Dublin, Ireland, 2018, pp. 1-25.

[9] W. Winter, K. Elkington and G. Bareux, "Pushing the limits: Europe's new grid: Innovative tools to combat transmission bottlenecks and reduced inertia," *IEEE Power and Energy Magazine*, vol. 13, no. 1, pp. 60-74, Dec. 2014.

[10] "9 August 2019 power outage report," Ofgem, Tech. Rep., Jan. 2020.

[11] "Update Report - Black System Event in South Australia on 28 September 2016," AEMO, Tech. Rep., 2016.

[12] P. Daly, D. Flynn and N. Cunniffe, "Inertia considerations within unit commitment and economic dispatch for systems with high non-synchronous penetrations," in *2015 IEEE Eindhoven PowerTech, Eindhoven*, Netherlands, 2015, pp. 1-6.

[13] A. Ulbig, T. S. Borsche and G. Andersson, "Impact of low rotational inertia on power system stability and operation," *IFAC Proceedings Volumes*, vol. 47, no. 3, pp. 7290-7297, 2014.

[14] J. De La Ree, V. Centeno, J. S. Thorp and A. G. Phadke, "Synchronized phasor measurement applications in power systems," *IEEE Trans. Smart Grid*, vol. 1, no. 1, pp. 20-27, Jun. 2010.

[15] S. You, *et al*., "Non-invasive identification of inertia distribution change in high renewable systems using distribution level PMU," *IEEE Trans. Power Sys.*, vol. 33, no. 1, pp. 1110-1112, Jan. 2018.

[16] B. K. Poolla, S. Bolognani and F. Dörfler, "Optimal placement of virtual inertia in power grids," *IEEE Trans. Automatic Control*, vol. 62, no. 12, pp. 6209-6220, Dec. 2017.

[17] E. Heylen, G. Strbac and F. Teng. "Challenges and opportunities of inertia estimation and forecasting in low-inertia power systems," *Renewable and Sustainable Energy Reviews*, vol. 147, pp. 111176, Sep. 2021.

[18] P. M. Ashton, C. S. Saunders and G. A. Taylor, "Inertia estimation of the GB power system using synchrophasor measurements," *IEEE Trans. Power Syst.*, vol. 30, no. 2, pp. 701-709, Mar. 2015.

[19] "EPIC 2.05: inertia response emulation for DG," Pacific Gas and Electric Company, Tech. Rep., 2019.

[20] T. Ujjwol *et al*., "Virtual inertia: current trends and future directions," *Applied Sciences*, vol. 7, no .7, pp. 654, 2017.

[21] P. Tielens, D. Van Hertem, "The relevance of inertia in power systems," *Renewable and Sustainable Energy Reviews*, vol. 55, pp. 999-1009, Mar. 2016.

[22] P. Kundur, *Power system stability and control*. New York, NY, USA: McGraw-Hill, 1994.

[23] A. Fernández-Guillamón, A. Vigueras-Rodríguez and Molina-García Á, "Analysis of power system inertia estimation in high wind power plant integration scenarios," *IET Renewable Power Generation*, vol. 13, no. 15, pp. 2807-2816, Nov. 2019.

[24] R. Shah, N. Mithulananthan and R. C. Bansal *et al*., "A review of key power system stability challenges for large-scale PV integration," *Renewable and Sustainable Energy Reviews*, Vol. 41, pp. 1423-1436, Jan. 2015.

[25] M. A. Abdullah, A. H. M. Yatim and C. W. Tan *et al*., "A review of maximum power point tracking algorithms for wind energy systems," *Renewable and sustainable energy reviews*, vol. 16, no. 5, pp. 3220-3227, Jun. 2012.

[26] J. Ram, Prasanth, T. Sudhakar Babu and N. Rajasekar, "A comprehensive review on solar PV maximum power point tracking techniques," *Renewable and Sustainable Energy Reviews*, vol. 67, pp. 826-847, Jan. 2017.

[27] J. Zhao, X. Lyu and Y. Fu *et al*., "Coordinated microgrid frequency regulation based on DFIG variable coefficient using virtual inertia and

primary frequency control," *IEEE Trans. Energy Conversion*, vol. 31, no. 3, pp. 833-845, Sep. 2016.
[28] J. J. Justo, F. Mwasilu and J. W. Jung, "Doubly-fed induction generator-based wind turbines: A comprehensive review of fault ride-through strategies," *Renewable and Sustainable Energy Reviews*, vol. 45, pp. 447-467, May. 2015.
[29] R. Ghosh, N. R. Tummuru and B. S. Rajpurohit *et al*., "Virtual inertia from renewable energy sources: mathematical representation and control strategy," in *2020 IEEE International Conference on Power Electronics, Smart Grid and Renewable Energy (PESGRE2020)*, Cochin, India, 2020, pp. 1-6.
[30] A. Fernández-Guillamón, E. Gómez-Lázaro and E. Muljadi, *et al.*, "Power systems with high renewable energy sources: A review of inertia and frequency control strategies over time," *Renewable and Sustainable Energy Reviews*, vol. 115, pp. 109369, Nov. 2019.
[31] N. Zhou, D. Meng and S. Lu, "Estimation of the dynamic states of synchronous machines using an extended particle filter," *IEEE Trans. on Power Syst.*, vol. 28, no.4, pp. 4152-4161, Jun. 2013.
[32] E. P. T. Cari, L. F. C. Alberto, "Parameter estimation of synchronous generators from different types of disturbances," in *2011 IEEE Power and Energy Society General Meeting*, Detroit, MI, USA, 2011, pp. 1-7.
[33] I. D. Ilina, "Experimental determination of moment to inertia and mechanical losses vs. speed, in electrical machines," in *2011 7th International Symposium on Advanced Topics in Electrical Engineering (ATEE)*, Bucharest, Romania, 2011, pp. 1-4.
[34] R. Babau, I. Boldea, T. J. E. Miller and N. Muntean, "Complete parameter identification of large induction machines from no-load acceleration–deceleration tests," *IEEE Trans. Industrial Electronics*, vol. 54, no. 4, pp. 1962-1972, Aug. 2007.
[35] T. Benšić, T. Varga, M. Barukčić, S. Križanić and V. JerkovićŠtil, "Identification of Inertia Constant from Induction Motor Load Transient," in *2019 International IEEE Conference and Workshop in Óbuda on Electrical and Power Engineering (CANDO-EPE)*, Budapest, Hungary, 2019, pp. 55-60.
[36] M. Namba, T. Nishiwaki and S. Yokokawa *et al*., "Idenntification of parameters for power system stability analysis using Kalman filter," *IEEE Trans. on Power Apparatus and Systems*, vol. PAS-100, no. 7, pp. 3304-3311, Jul. 1981.
[37] M. Burth, G. C. Verghese and M. Velez-Reyes, "Subset selection for improved parameter estimation in on-line identification of a synchronous generator," *IEEE Trans. Power Syst.*, vol. 14, no. 1, pp. 218-225, Feb. 1999.
[38] Y. Wehbe, L. L Fan and Z. X. Miao, "Least squares-based estimation of synchronous generator states and parameters with phasor measurement units," in *2012 North American Power Symposium (NAPS)*, Champaign, IL, USA, 2012, pp. 1-6.
[39] E. P. T. Cari and L. F. C. Alberto, "Parameter estimation of synchronous generators from different types of disturbances," in *Power & Energy Society General Meeting*, Detroit, MI, USA, 2011, pp. 1-7.
[40] M. Huang, Li W, Yan W, "Estimating parameters of synchronous generators using square-root unscented Kalman filter," *Electric Power Systems Research*, vol. 80, no. 9, pp. 1137-1144, Sep. 2010.
[41] A. Rouhani and A. Abur, "Constrained iterated unscented Kalman filter for dynamic state and parameter estimation," *IEEE Trans. on Power Syst.*, vol. 33, no. 3, pp. 2404-2414, May 2018.
[42] D. G. Del, S. Grillo, "Analysis of the sensitivity of extended Kalman filter-based inertia estimation method to the assumed time of disturbance," *Energies*, vol. 12, no. 3, pp. 483, 2019.
[43] H. G. Aghamolki, Z. Miao, L. Fan *et al*., "Identification of synchronous generator model with frequency control using unscented Kalman filter," *Electric Power Systems Research*, vol. 126, pp. 45-55, Sep. 2015.
[44] L. Fan, Y. Wehbe, "Extended Kalman filtering based real-time dynamic state and parameter estimation using PMU data," *Electric Power Systems Research*, vol. 103, pp. 168-177, Oct. 2013.
[45] M. A. Gonzalez-Cagigal, J. A. Rosendo-Macias, and A. Gomez-Exposito, "Parameter estimation of fully regulated synchronous generators using Unscented Kalman Filters," *Electric power systems research*, vol. 168, pp. 210-217, Mar. 2019.
[46] G. Valverde, E. Kyriakides and G. T. Heydt *et al.*, "Nonlinear estimation of synchronous machine parameters using operating data," *IEEE Trans. Energy Conversion*, vol. 26, no. 3, pp. 831-839, Sep. 2011.
[47] E. L. Geraldi, T. C. C. Fernandes and R. A. Ramos, "A UKF-based approach to estimate parameters of a three-phase synchronous generator model," *Energy Systems*, vol. 9, no. 3, pp. 1-31, 2018.
[48] E. L. Geraldi, T. C. C. Fernandes, A. B. Piardi, *et al.*, "Parameter estimation of a synchronous generator model under unbalanced operating conditions," *Electric Power Systems Research*, vol. 187, pp. 106487, Oct. 2020.
[49] A. Vahidnia, G. Ledwich, E. Palmer, *et al.*, "Generator coherency and area detection in large power systems," *IET Generation, Transmission & Distribution*, vol. 6, no. 9, pp. 874-883, Sep. 2012.
[50] P. Ju, L. Q. Ni and F. Wu, "Dynamic equivalents of power systems with online measurements. Part 1: theory," *IEE Proceedings-Generation, Transmission and Distribution*, vol. 151, no. 2, pp. 175-178, Mar. 2004.
[51] P. Ju, F. Li, N. G. Yang, *et al*., "Dynamic equivalents of power systems with online measurements Part 2: applications," *IEE Proceedings-Generation, Transmission and Distribution*, vol. 151, no. 2, pp. 179-182, Mar. 2004.
[52] A. Chakrabortty, J. H. Chow, A. Salazar, "A measurement-based framework for dynamic equivalencing of large power systems using wide-area phasor measurements," *IEEE Trans. on Smart Grid*, vol. 2, no. 1, pp. 68-81, March 2011.
[53] M. Shiroei, B. Mohammadi-Ivatloo and M. Parniani, "Low-order dynamic equivalent estimation of power systems using data of phasor measurement units," *International Journal of Electrical Power & Energy Systems*, vol.74, pp. 134-141, Jan. 2016.
[54] S. Nabavi, A. Chakrabortty, "Structured identification of reduced-order models of power systems in a differential-algebraic form," *IEEE Trans. on Power Syst.*, vol. 32, no. 1, pp. 198-207, Jan. 2017.
[55] G. Cai, B. Wang, D. Yang, *et al.*, "Inertia estimation based on observed electromechanical oscillation response for power systems," *IEEE Trans. Power Syst.*, vol. 34, no. 6, pp. 4291-4299, Nov. 2019.
[56] D. Yang, B. Wang, G. Cai, *et al*., "Data-driven estimation of inertia for multi-area interconnected power systems using dynamic mode decomposition," *IEEE Trans. Industrial Informatics*, vol. 17, no. 4, pp. 2686-2695, Apr. 2021.
[57] A. T. Sarić, M. T. Transtrum, A. M. Stanković, "Data-driven dynamic equivalents for power system areas from boundary measurements," *IEEE Trans. Power Syst.*, vol. 34, no. 1, pp. 360-370, Jan. 2019.
[58] F. Milano, "A method for evaluating frequency regulation in an electrical grid part I: theory," *IEEE Trans. Power Syst.*, vol. 36, no. 1, pp. 183-193, Jan. 2021.
[59] F. Milano, "A method for evaluating frequency regulation in an electrical grid part II: applications to non-synchronous devices," *IEEE Trans. Power Syst.*, vol. 36, no. 1, pp. 194-203, Jan. 2021.
[60] F. Milano, O. Alvaro, "Frequency divider," *IEEE Trans. Power Syst.*, vol. 32, no. 2, pp. 1493-1501, Mar. 2017.
[61] V. Terzija *et al*., "Wide-area monitoring, protection, and control of future electric power networks," *Proceedings of the IEEE*, vol. 99, no. 1, pp. 80-93, Jan. 2011.
[62] J. Zhao, Y. Tang and V. Terzija, "Robust online estimation of power system center of inertia frequency," *IEEE Trans. Power Syst.*, vol. 34, no. 1, pp. 821-825, Jan. 2019.
[63] D. Zografos, M. Ghandhari, "Power system inertia estimation by approaching load power change after a disturbance," in *2017 IEEE Power & Energy Society General Meeting*, Chicago, IL, USA, 2017, pp. 1-5.
[64] A. Riepnieks and H. Kirkham, "Rate of change of frequency measurement," in *2016 57th International Scientific Conference on Power and Electrical Engineering of Riga Technical University (RTUCON)*, Riga, Latvia, 2016, pp. 1-5.
[65] T. Inoue, H. Taniguchi, Y. Ikeguchi, *et al.*, "Estimation of power system inertia constant and capacity of spinning-reserve support generators using measured frequency transients," *IEEE Trans. Power Syst.*, vol. 12, no. 1, pp. 136-143, Feb. 1997.
[66] P. Du, Y. Makarov, "Using disturbance data to monitor primary frequency response for power system interconnections," *IEEE Trans. Power Syst.*, vol. 29, no. 3, pp. 1431-1432, May. 2014.
[67] P. M. Ashton, G. A. Taylor, A. M. Carter, *et al*., "Application of phasor measurement units to estimate power system inertial frequency response," in *2013 IEEE Power & Energy Society General Meeting*, Vancouver, BC, Canada, 2013, pp. 1-5.
[68] C. Phurailatpam, Z. H. Rather, B. Bahrani, *et al*., "Measurement based estimation of inertia in AC microgrids," *IEEE Trans. Sustainable Energy*, vol. 11, no. 3, pp. 1975-1984, Jul. 2020.
[69] M. Sun, Y. Feng, P. Wall, *et al*., "On-line power system inertia calculation using wide area measurements," *International Journal of Electrical Power & Energy Systems*, vol. 109, pp. 325-331, Jul. 2019.

[70] R. K. Panda, A. Mohapatra, S. C. Srivastava, "Online estimation of system inertia in a power network utilizing synchrophasor measurements," *IEEE Trans. Power Syst.*, vol. 35, no. 4, pp. 3122-3132, Jul. 2020.

[71] D. P. Chassin, Z. Huang, M. K. Donnelly, *et al*., "Estimation of WECC system inertia using observed frequency transients," *IEEE Trans. Power Syst.*, vol. 20, no. 2, pp. 1190-1192, May. 2005.

[72] P. M. Ashton, C. S. Saunders, G. A. Taylor, *et al*., "Inertia estimation of the GB power system using synchrophasor measurements," *IEEE Trans. Power Syst.*, vol. 30, no. 2, pp. 701-709, Mar. 2015.

[73] P. Wall, F. Gonzalez-Longatt, V. Terzija, "Estimation of generator inertia available during a disturbance," in *2012 IEEE Power and Energy Society General Meeting*, San Diego, CA, USA, 2012, pp. 1-8.

[74] P. Wall, V. Terzija, "Simultaneous estimation of the time of disturbance and inertia in power systems," *IEEE Trans. Power Delivery*, vol. 29, no. 4, pp. 2018-2031, Aug. 2014.

[75] D. Zografos, M. Ghandhari, "Estimation of power system inertia," in *2016 IEEE Power and Energy Society General Meeting (PESGM)*, Boston, MA, USA, 2016, pp. 1-5.

[76] Y. Zhang, J. Bank, Y. H. Wan, *et al*., "Synchrophasor measurement-based wind plant inertia estimation," in *2013 IEEE Green Technologies Conference (GreenTech)*, Denver, CO, USA, 2013, pp. 494-499.

[77] D. Wilson, J. Yu, N. Al-Ashwal, *et al*., "Measuring effective area inertia to determine fast-acting frequency response requirements," *International Journal of Electrical Power and Energy Systems*, vol. 113. pp. 1-8, Dec. 2019.

[78] D. Zografos, M. Ghandhari, "Power system inertia estimation by approaching load power change after a disturbance," in *2017 IEEE Power & Energy Society General Meeting*, Chicago, IL, USA, 2017, pp. 1-5.

[79] D. Zografos, M. Ghandhari, R. Eriksson. "Power system inertia estimation: Utilization of frequency and voltage response after a disturbance," Electric Power Systems Research, vol.161, pp. 52-60, Aug. 2018.

[80] V. S. Perić, L. Vanfretti, "Power-system ambient-mode estimation considering spectral load properties," *IEEE Trans. Power Syst.*, vol. 29, no. 3, pp. 1133-1143, May. 2014.

[81] L. Vanfretti, L. Dosiek, J. W. Pierre, *et al*., "Application of ambient analysis techniques for the estimation of electromechanical oscillations from measured PMU data in four different power systems," *European Transactions on Electrical Power*, vol. 21, no. 4, pp. 1640-1656, May. 2011.

[82] X. Cao, B. Stephen, I. F. Abdulhadi, *et al*., "Switching Markov Gaussian models for dynamic power system inertia estimation," *IEEE Trans. Power Syst.*, vol. 31, no. 5, pp. 3394-3403, Sep. 2016.

[83] K. Tuttelberg, J. Kilter, D. Wilson, *et al*., "Estimation of power system inertia from ambient wide area measurements," *IEEE Trans. Power Syst.*, vol. 33, no. 6, pp. 7249-7257, Nov. 2018.

[84] J. Zhang, H. Xu, "Online identification of power system equivalent inertia constant," *IEEE Trans. Industrial Electronics*, vol. 64, no. 10, pp. 8098-8107, Oct. 2017.

[85] J. Schiffer, P. Aristidou and R. Ortega, "Online estimation of power system inertia using dynamic regressor extension and mixing," *IEEE Trans. Power Syst.*, vol. 34, no. 6, pp. 4993-5001, Nov. 2019.

[86] D. Yang, B. Wang, J. Ma *et al*., "Ambient-data-driven modal-identification-based approach to estimate the inertia of an interconnected power system," *IEEE Access*, vol. 8, pp. 118799-118807, 2020.

[87] F Zeng, J Zhang, G Chen, et al., "Online estimation of power system inertia constant under normal operating conditions," *IEEE Access*, vol. 8, pp. 101426-101436, 2020.

[88] F. Zeng, J Zhang, Y Zhou *et al*., "Online identification of inertia distribution in normal operating power system," *IEEE Trans. Power Syst.*, vol. 35, no. 4, pp. 3301-3304, Jul. 2020.

[89] J. Zhao, M. Netto, Z. Huang, *et al*., "Roles of dynamic state estimation in power system modeling, monitoring and operation," *IEEE Trans. on Power Syst.*, vol. 36, no. 3, pp. 2462-2472, May. 2021 .

[90] "Benchmark systems for small-signal stability analysis and controls, power system dynamic performance," IEEE PES Task Force, Piscataway, NJ, USA, Tech. Rep. PES-TR18, Aug. 2015.

[91] Y. Cheng, R. Azizipanah-Abarghooee, S. Azizi. *et al.*, "Smart frequency control in low inertia energy systems based on frequency response techniques: A review," *Applied Energy*, vol. 279, pp. 115798, 2020.

[92] D. Sun, H. Liu, S. Gao, L. Wu, P. Song and X. Wang, "Comparison of different virtual inertia control methods for inverter-based generators," *Journal of Modern Power Systems and Clean Energy*, vol. 8, no. 4, pp. 768-777, Jul. 2020.

[93] A. Ortega, F. Milano, "Comparison of different PLL implementations for frequency estimation and control," in *18th International Conference on Harmonics and Quality of Power*, Ljubljana, Slovenia, May. 2018, pp. 1-6.

[94] J. Van de Vyver, J. D. M. De Kooning, B. Meersman, *et al*., "Droop control as an alternative inertial response strategy for the synthetic inertia on wind turbines," *IEEE Trans. on Power Syst.*, vol. 31, no. 2, pp. 1129-1138, Mar. 2016.

[95] Z. S. Zhang, Y. Z. Sun, J. Lin, *et al*., "Coordinated frequency regulation by doubly fed induction generator-based wind power plants," *IET Renewable Power Generation*, vol. 6, no. 1, pp. 38-47, Jan. 2012.

[96] M. Hwang, E. Muljadi, J. W. Park, *et al*., "Dynamic droop–based inertial control of a doubly-fed induction generator," *IEEE Trans. Sustainable Energy*, vol. 7, no. 3, pp. 924-933, Jul. 2016.

[97] K. V. Vidyanandan, N. Senroy, "Primary frequency regulation by deloaded wind turbines using variable droop," *IEEE Trans. on Power Syst.*, vol. 28, no. 2, pp. 837-846, May 2013.

[98] C. Gavriluta, I. Candela, J. Rocabert, *et al*., "Storage system requirements for grid supporting PV-power plants," in *2014 IEEE Energy Conversion Congress and Exposition (ECCE)*, Pittsburgh, PA, USA, 2014, pp. 5323-5330.

[99] H Liao, X Zhang and X Hou, "A decentralized control of series-connected PV-ES inverters with MPPT and virtual inertia functionality," in *2020 IEEE Applied Power Electronics Conference and Exposition (APEC)*, New Orleans, LA, USA, 2020, pp. 3221-3224.

[100] J. G. Ramos, R. E. Araújo, "Virtual inertia and droop control using DC-link in a two-stage PV inverter," in *2020 IEEE 14th International Conference on Compatibility, Power Electronics and Power Engineering (CPE-POWERENG)*, Setubal, Portugal, 2020, pp. 55-60.

[101] J. Khazaei, Z. Tu and W. Liu, "Small-signal modeling and analysis of virtual inertia-based PV systems," *IEEE Trans. Energy Conversion*, vol. 35, no. 2, pp. 1129-1138, Jun. 2020.

[102] S. I. Nanou, A. G. Papakonstantinou, S. A. Papathanassiou, "A generic model of two-stage grid-connected PV systems with primary frequency response and inertia emulation," *Electric Power Systems Research*, vol. 127, pp. 186-196, Oct. 2015.

[103] R. H. Lasseter, Z. Chen, D. Pattabiraman, "Grid-forming inverters: a critical asset for the power grid," *IEEE Journal of Emerging and Selected Topics in Power Electronics*, vol. 8, no. 2, pp. 925-935, Jun. 2020.

[104] J. Liu, Y. Miura and T. Ise, "Comparison of Dynamic Characteristics Between Virtual Synchronous Generator and Droop Control in Inverter-Based Distributed Generators," *IEEE Trans. Power Electronics*, vol. 31, no. 5, pp. 3600-3611, May. 2016.

[105] Q. C. Zhong, P. L. Nguyen, Z. Ma, *et al*., "Self-synchronized synchronverters: Inverters without a dedicated synchronization unit," *IEEE Trans. Power Electronics*, vol. 29, no. 2, pp. 617-630, Feb. 2014.

[106] W. Zhang, D. Remon, P. Rodriguez, "Frequency support characteristics of grid-interactive power converters based on the synchronous power controller," *IET Renewable Power Generation*, vol. 11, no. 4, pp. 470-479, 2016.

[107] J. Alipoor, Y. Miura and T. Ise, "Distributed generation grid integration using virtual synchronous generator with adoptive virtual inertia," in *2013 IEEE Energy Conversion Congress and Exposition*, Denver, CO, USA, 2013, pp. 4546-4552.

[108] J Alipoor, Y Miura and T Ise, "Power system stabilization using virtual synchronous generator with alternating moment of inertia," *IEEE Journal of Emerging and Selected Topics in Power Electronics*, vol. 3, no. 2, pp. 451-458, June 2015.

[109] D. Li, Q. Zhu, S. Lin, *et al.*, "A self-adaptive inertia and damping combination control of VSG to support frequency stability," *IEEE Trans. Energy Conversion*, vol. 32, no. 1, pp. 397-398, Mar. 2017.

[110] R. Shi, X. Zhang, C. Hu *et al*., "Self-tuning virtual synchronous generator control for improving frequency stability in autonomous photovoltaic-diesel microgrids," *Journal of Modern Power Systems and Clean Energy*, vol. 6, no. 3, pp. 482-494, May 2018.

[111] Shrestha Pratigya. Inverter-based control to enhance the resiliency of a distribution system. Ph.D. dissertation, Virginia Tech, Blacksburg, VA, USA, 2019.

[112] H. U. Rehman, X. Yan, M. A. Abdelbaky, *et al*., "An advanced virtual synchronous generator control technique for frequency regulation of grid-connected PV system," *International Journal of Electrical Power & Energy Systems*, vol. 125, pp. 106440, Feb. 2021.

[113]Y. Ma, L. Yang, F. Wang, L. M. Tolbert, "Voltage closed-loop virtual synchronous generator control of full converter wind turbine for grid-connected and stand-alone operation," in *2016 IEEE Applied Power Electronics Conference and Exposition (APEC)*, Long Beach, CA, USA, 2016, pp. 1261-1266.

[114]S. Yu, K. Emami, T. Fernando, H. H. C. Iu, and K. P. Wong, "State estimation of doubly fed induction generator wind turbine in complex power systems," *IEEE Trans. Power Syst.*, vol. 31, no. 6, pp. 4935–4944, Nov. 2016.

[115]S. Yu, T. Fernando, H. H. Iu, and K. Emami, "Realization of state estimation-based DFIG wind turbine control design in hybrid power systems using stochastic filtering approaches," *IEEE Trans. Industrial Informatics*, vol. 12, no. 3, pp. 1084–1092, Jun. 2016.

[116]S. S. Yu *et al*., "An unscented particle filtering approach to decentralized dynamic state estimation for DFIG wind turbines in multi-area power systems," *IEEE Trans. Power Syst.*, vol. 35, no. 4, pp. 2670–2682, Jul. 2020.

[117]G. Anagnostou, L. P. Kunjumuhammed, and B. C. Pal, "Dynamic state estimation for wind turbine models with unknown wind velocity," *IEEE Trans. Power Syst.*, vol. 34, no. 5, pp. 3879–3890, Sep. 2019.

[118]Y Susuki, A Chakrabortty, "Introduction to Koopman mode decomposition for data-based technology of power system nonlinear dynamics," *IFAC-PapersOnLine*, vol. 51, no. 28, pp. 327-332, 2018.

[119]D. Huang *et al*., "An analytical method for disturbance propagation investigation based on the electromechanical wave approach," *IEEE Trans. Power Syst.*, vol. 36, no. 2, pp. 991-1001, Mar. 2021.

[120]E. S. N. R. Paidi et al., "Development and Validation of Artificial Neural Network-Based Tools for Forecasting of Power System Inertia With Wind Farms Penetration," *IEEE Systems Journal*, vol. 14, no. 4, pp. 4978-4989, Dec. 2020